Hindawi
International Transactions on Electrical Energy Systems
Volume 2022, Article ID 3970536, 12 pages
https://doi.org/10.1155/2022/3970536

*Research Article*

# Resilience Assessment for Microgrid with Pre-Position and Reconfiguration of Emergency Distribution Generations under Natural Hazard

**Hongtao Lei**,[1,2] **Shengjun Huang**,[1,2] **Yajie Liu**,[1,2] **and Tao Zhang**[1,2]

[1]*College of Systems Engineering, National University of Defense Technology, Changsha, Hunan 410073, China*
[2]*Hunan Key Laboratory of Multi-Energy System Intelligent Interconnection Technology, Changsha, Hunan 410073, China*

Correspondence should be addressed to Hongtao Lei; hongtaolei@aliyun.com

Received 3 March 2022; Revised 23 March 2022; Accepted 30 March 2022; Published 15 April 2022

Academic Editor: Qiuye Sun



Recently, increasing the number and severity of the natural hazards requires the resilience assessment and enhancement of the power system, especially the microgrid system. The emergency distribution generations have great potential to enhance the resilience of microgrid against blackouts under the emergency environment. This paper investigates the resilience assessment of the microgrid system under natural hazard, where emergency distribution generations are firstly pre-positioned on system nodes and then reconfigured after system damage occurs. A new resilience metric index and an efficient approximation computation method are provided for the resilience assessment of the focused problem. A new pre-position strategy and a new reconfiguration strategy on emergency distribution generations are proposed for the microgrid system emergency restoration under natural hazard. Also, a framework of resilience assessment is provided for problem-solving. The results of extensive experiments on the modified IEEE 30-Bus system and modified IEEE 118-Bus system confirm the effectiveness of the resilience assessment methodology and the superiority of proposed restoration strategies.

## 1. Introduction

Due to a lot of the blackouts caused by natural hazards, the resilience of power systems has become a focusing point in society nowadays. As a smart terminal end of the power grid, the microgrid system provides the services of power supply for domestic and industrial customers, and the resilience of microgrid closely corresponds to the quality of services for the customers. However, the extreme disruptions under natural hazards, which lead to line failure, equipment damage, infrastructure destruction, and so on, would result in large-scale outages and loss of health and wealth. For example, in the US, natural hazards cause about 25 to 70 billion dollars to cost annually [1]. Therefore, it is necessary to assess and improve the power system resilience under natural hazards, especially for the microgrid system.

In the literature, Holling [2] firstly introduced the concept of resilience from a view of the ecological system, where it defined the resilience of the ecological system as its ability to move away from equilibria for disturbances. Then, a lot of research works on resilience in the social system [3], engineering system [4], and so on have been triggered. Like Mili et al. [5], in this work, we consider resilience as the ability of a system, where the system performance degrades for unexpected extreme disturbances and the system could recover its function through emergency restoration actions once the disturbances cease. Since the focus on the resilience of power system to extreme events is increasing, it is important to develop the related quantitative approaches and metrics for the measure of resilience. Several resilience metrics have been provided in [6–12]. Bruneau et al. [7] introduced a "resilience triangle" to assess seismic resilience of community system, where the resilience can be computed as the integral of degraded system performance with time after disruptions [13]. Ouyang and Duenas-Osorio [11] proposed the time-dependent resilience metrics for urban infrastructure systems. Also, Panteli et al. [12] proposed a "resilience trapezoid" metric concept, during which authors

extended the "resilience triangle" to fix the different phase measure of system resilience for the disruption. Lei et al. [14] proposed a two-stage dispatch framework consisting of pre-positioning and real-time allocation for dispatching mobile emergency generators as distributed generators in distribution systems to restore critical loads by forming multiple microgrids. Ti et al. [15] provided a cyber-physical power system resilience assessment framework that considered the space-time metrics of disasters. A state-of-the-art review of existing research on the study of grid resilience for definitions, frameworks, quantitative assessment methodologies, and enhancement strategies has been presented by Jufri et al. [10]. Also, an overview of the assessment metrics of the concept of resilience in electrical grids was given by Dehghani et al. [8], who explained the metrics that have been presented in various researches and compared these metrics from different aspects in order to determine the most comprehensive metric.

For microgrid, Amirioun et al. [16] presented a microgrid proactive management framework to cope with adverse impacts of extreme windstorms, and the proposed method considered the benefit of network reconfiguration, generation reschedule, backup generation capacity, and so on. Amirioun et al. [6] provided a quantitative framework for assessing the system resilience in response to high-impact low-probability windstorms, where the proposed framework jointly employs fragility curves of overhead distribution branches and windstorm profile to quantify the degradation in microgrid performance. Hussain et al. [17] reviewed the formation and strategy of microgrids for resilience enhancement and provided future directions for resilience-oriented operation methods. Nelson et al. [18] developed a statistical framework to quantify resilience of grid-connected microgrids to ensure critical loads served during islanding scenarios, and Markov chains were used to evaluate microgrid transition states for the quantified resilience. Ibrahim and Alkhraibat [9] introduced a set of metrics that are utilized for resiliency quantification of microgrid systems, such as level of resilience, level of performance reduction, and recovery time.

In summary, the aforementioned work focuses on either power system's (or microgrid) general resilience assessment or enhancement method under extreme disturbances, where the system resilience assessment and enhancement problems are considered simultaneously. However, different from the above research work, (1) we consider the resilience assessment for the microgrid with system emergency restoration under natural hazard, where the resilience emergency enhancement strategies in the predisturbance and restoration phases are incorporated into the resilience assessment progress; (2) we extend the system resilience metric of microgrid with consideration of the supplied load demand importance and propose an efficient approximation computation method for the resilience metric index based on the system emergency restoration strategy; (3) we also provide a new pre-position strategy and a new reconfiguration strategy on emergency distribution generations for microgrid system restoration, considering the flexibility and practicability of microgrid restoration action under the emergency environment. So, the main contributions of this paper are summarized as follows:

(i) To the best of our knowledge, the emergency system restoration with distribution generation has never been considered in the resilience assessment for the microgrid under natural hazard. This gap is filled by this paper.

(ii) In this new problem, the emergency distribution generations are pre-positioned and reconfigured on the microgrid nodes for emergency system restoration. A new resilience metric index with the integration of load demand importance and system resilience is provided for the resilience assessment of the proposed problem. An efficient approximation computation method is presented for the proposed resilience metric index, based on the system restoration strategy.

(iii) A new pre-position strategy and a new reconfiguration strategy for emergency distribution generations are proposed for the improvement of system resilience and performance at the stage of system restoration. An assessment framework of the focused problem is also provided for the problem-solving.

(iv) The effectiveness of the resilience assessment methodology and the superiority of the restoration strategies are demonstrated in the extensive experiments on the modified IEEE 30-Bus system and modified IEEE 118-Bus system.

The remainder of the paper is structured as follows. Section 2 describes the focused problem and provides the resilience metric for this paper. Section 3 presents the fragility modeling under hazard, the emergency system restoration with distribution generation pre-position and reconfiguration, the computation of resilience metric under emergency system restoration, and the assessment framework for the methodology. Results of simulation experiments are discussed in Section 4. Section 5 concludes the paper.

## 2. Problem Description and Resilience Metric

The focused issue is to assess the system resilience for the microgrid under hazard, where emergency distribution generations are pre-positioned and reconfigured on microgrid nodes for the emergence system restoration. There exist two stages for the system restoration: (1) the distribution generations are first pre-positioned on nodes as backups before the hazard event; (2) after the hazard occurs, the pre-positioned generations are reconfigured to the suitable nodes for maximal system resilience and performance.

The hazard, for example, windstorm, earthquake, flood, and so on, causes the performance of the microgrid system to be degraded by destroying its elements such as transmission lines, electric transformers, and plants. Since the repair for the destroyed elements of the power system

requires the collection of equipment resources and repair crews, it usually needs to be implemented for several hours (or even several days) after the hazard happens, which may lead to the huge cost of economy and health. Therefore, the emergency distribution generations, such as microturbine and mobile energy storage system, are pre-positioned and reconfigured on microgrid nodes, respectively, before and after the hazard for rapid and efficient system restoration.

In this paper, there exist a microgrid node set $N = \{1, \ldots, i, \ldots n\}$ and a distribution generation set $M = \{1, \ldots, k, \ldots, m\}$, where $m < n$ and distribution generation $k$ has capacity $G_k$. The concerned conceptual resilience curve is shown in Figure 1. The microgrid states include six states, which are the predisturbance state $[t_0, t_e]$, the degradation state $[t_e, t_{de}]$, the degraded state $[t_{de}, t_{re}]$, the restoration state $[t_{de}, t_{\text{res}}]$, the restored state $[t_{\text{res}}, t_{ir}]$, and the infrastructure recovery state $[t_{ir}, t_{\text{pir}}]$. In Figure 1, a hazard event happens at $t_e$, which results in the performance degradation of the microgrid in $[t_e, t_{de}]$. After the event, the damage and consequences are identified to preserve the optimal operation of the microgrid system in $[t_{de}, t_{re}]$, and the performance of the microgrid stays at a postevent degraded level $Q_{de}$.

During the restoration progress of $[t_{re}, t_{\text{res}}]$, the pre-positioned or reconfigured emergency distribution generations are sequentially added to the microgrid for rapid and efficient energy supplying, considering the system stability and demand of critical loads. After the emergency system restoration, the performance of the microgrid will be improved to an upgraded level $Q_{re}$. The level $Q_{re}$ could be higher or less than the predisturbance system performance level $Q_0$, which depends on the system restoration actions and the capacities of emergency distribution generations. Note that, for convenience and simplicity, we believe that, at each "pre-" or "-ed" state in Figure 1, the microgrid system will achieve optimal stable performance under its situation.

In Figure 1, we consider three cases for the value of upgraded level $Q_{re}$, described as $C_0$"$C_0$," "$C_1$," and "$C_2$," respectively. The remarkable unsatisfied demands have been considered at the predisturbance state, and enough emergency distribution generations have been added at the restoration state in the case of $C_2$"$C_2$," so it obtains a final performance higher than that of the predisturbance state. The microgrid system remains at the upgraded level $Q_{re}$ for the emergency restoration actions in $[t_{\text{res}}, t_{ir}]$. Then, the infrastructure recovery will be implemented from $t_{ir}$ to $t_{\text{pir}}$. This paper focuses on period horizon $T$ from $t_e$ to $t_{ir}$, which involves the degradation state, degraded state, restoration state, and restored state.

System resilience is a system's ability to prepare for and adapt to changing conditions and withstand and recover rapidly from disruptions [19]. And the load shedding has been widely considered as the disturbance which directly impacts the system restoration process [20]. The microgrid system performance can be defined as the load demand supplied at the period horizon $T$, and then the microgrid system resilience in this work is quantified based on the percentage of the met demand with consideration of the supplied load weight as follows:

$$R = \frac{\int_{t_e}^{t_{ir}} \sum_{i \in N} w_i q_i^1(t)\mathrm{d}t}{\int_{t_e}^{t_{ir}} \sum_{i \in N} w_i q_i^0(t)\mathrm{d}t} = \frac{\int_{t_e}^{t_{ir}} \sum_{i \in N} w_i q_i^1(t)\mathrm{d}t}{\sum_{i \in N} w_i q_i^0 T}, \tag{1}$$

where $N$ is the node set of the microgrid system, $q_i^0$ is the supplied load at node $i$ in $[t_0, t_e]$, $q_i^1(t)$ is the supplied load at node $i$ in $[t_e, t_{ir}]$, and $w_i$ is the weight of supplied load at node $i$. We can record $\sum_{i \in N} w_i q_i^0$ as $Q_i^0$ and $\sum_{i \in N} Q_i^0 = Q_0$, where the "weighted" supplied loads are considered as the "weighted" performance of the microgrid system at the predisturbance state. Also, $Q_{re}$ and $Q_{de}$ are the "weighted" performance of the microgrid system at their states. $\sum_{i \in N} w_i q_i^1(t)$ can be noted as $Q_i^1(t)$ and $\sum_{i \in N} Q_i^1(t) = Q^1(t)$. However, $Q^1(t)$ equals $Q_{de}$ and $Q_{re}$, respectively, at the degraded state and the restorated state, and the value depiction of $Q^1(t)$ at the degradation state and restoration state, respectively, corresponds to the descent curve and ascent curve. Then, formula (1) can be changed to

$$R = \int_{t_e}^{t_{ir}} \frac{Q^1(t)\mathrm{d}t}{Q_0 T} = \frac{\left(\int_{t_e}^{t_{de}} Q^1(t)\mathrm{d}t + Q_{de}(t_{re} - t_{de}) + \int_{t_{re}}^{t_{\text{res}}} Q^1(t)\mathrm{d}t + Q_{re}(t_{ir} - t_{\text{res}})\right)}{Q_0 T}. \tag{2}$$

In formula (2), two terms "$\int_{t_e}^{t_{de}} Q^1(t)\mathrm{d}t$" and "$\int_{t_{re}}^{t_{\text{res}}} Q^1(t)\mathrm{d}t$" are not easy to be computed. Referring to Panteli et al. [12] and Panteli et al. [21], we approximate "$\int_{t_e}^{t_{de}} Q^1(t)\mathrm{d}t$" as the sum of corresponding "triangle" and "rectangle" areas in Figure 1,

$$\int_{t_e}^{t_{de}} Q^1(t)\mathrm{d}t = \frac{(t_{de} - t_e)(Q_0 - Q_{de})}{2 + (t_{de} - t_e)Q_{de}}. \tag{3}$$

The term "$\int_{t_{re}}^{t_{\text{res}}} Q^1(t)\mathrm{d}t$" corresponds to the performance area of the microgrid system at the restoration state. For the stability of the microgrid system, we assume in the system restoration process that the pre-positioned and reconfigured emergency distribution generations are sequentially added to the system at each time interval $\Delta t$. The position and addition sequence of emergency distribution generations are important for system resilience assessment and affect the computation of $\int_{t_{re}}^{t_{\text{res}}} Q^1(t)\mathrm{d}t$"$\int_{t_{re}}^{t_{\text{res}}} Q^1(t)\mathrm{d}t$." We will discuss them in detail in Sections 3.2 and 3.3.

The values of $Q_0$"$Q_0$," "$Q_{de}$," and "$Q_{re}$" can be easily obtained by an optimal power flow (OPF) approach [22] based on the states of the microgrid system, where the focus of this work is on developing and illustrating a novel and specific resilience assessment methodology. It is worth mentioning that, based on the above discussion of computation and description of Figure 1, the value of the system

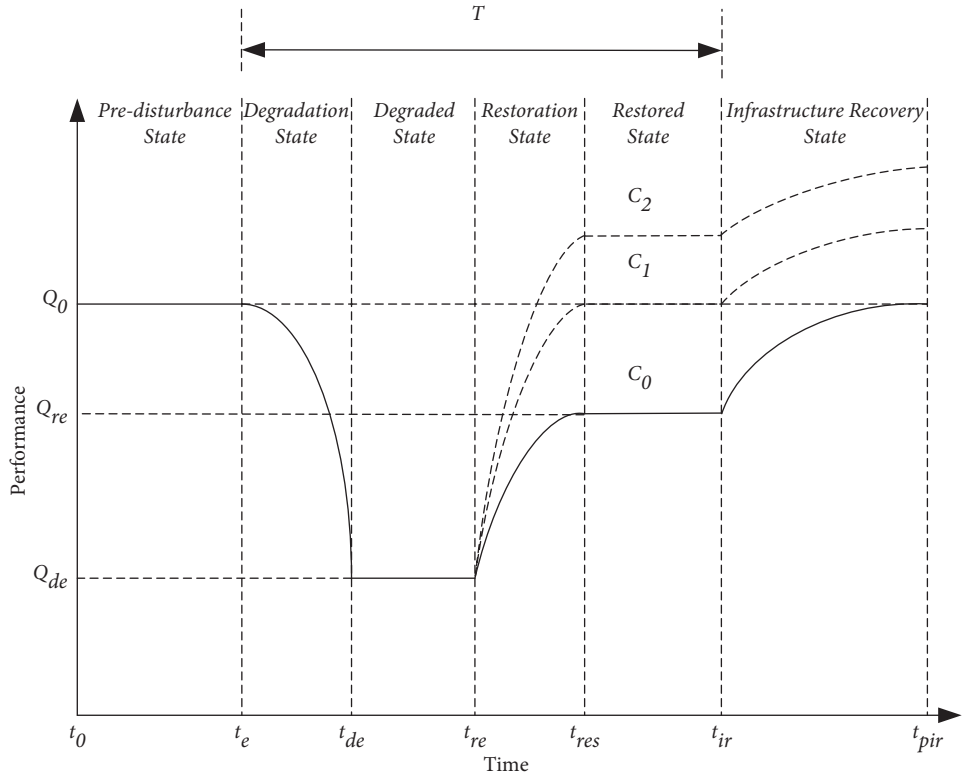


Figure 1: A conceptual resilience curve with a disturbance event and emergency restoration.

resilience metric "$R$" could be equal to 1, less than 1, or larger than 1.

## 3. Assessment Methodology for the Microgrid under Hazard

In this section, we provide an assessment methodology for the microgrid system with pre-position and reconfiguration of emergency distribution generations under hazard.

*3.1. Fragility Modeling under Hazard.* The fragility describes the failure of a structure or structural component of the focused system, conditional on a loading that relates to the potential intensity of a hazard [23]. The wind storm has been recognized to cause the highest percentage of failure in power infrastructure among hazards [24]. Therefore, we use it to model the fragility of the microgrid system under hazard, where the fragility modeling for other hazards is similar. Since the microgrid is geographically small, wind storm passes through the system within a few minutes, and we only consider the transmission line failure in the fragility modeling of the microgrid for simplicity. Like Panteli et al. [12]; Panteli et al. [23]; Panteli et al. [21]; Fu et al. [25]; and Amirioun et al. [6], we use the fragility curve that presents the failure probability of transmission line as a function of hazard intensity (e.g., wind speed) to model the fragility of transmission lines in microgrid system. We also apply the fragility curve shown in Figure 2, as Panteli et al. [12], with the following constraint.where $P_k(V)$ is the failure probability of transmission lines as a function of wind speed $V$ at simulation iteration $k$, $V_{\text{critical}}$ is the wind speed value at which the failure probability of lines can be discerned, and $V_{\text{collapse}}$ is the wind speed value when the failure of lines will certainly occur. For each transmission line, a uniformly distributed random number $u \in (0, 1)$ will be generated to check the failure of the line in each simulation iteration. If $P_k(V) > u$, the transmission line is not failed; otherwise, the transmission line is destroyed by the wind storm.

$$P_k(V) = \begin{cases} 0, & \text{if } V < V_{\text{critical}}, \\ P(V), & \text{if } V_{\text{critical}} \le V < V_{\text{collapse}}, \\ 1, & \text{if } V \ge V_{\text{collapse}}, \end{cases} \tag{4}$$

*3.2. Pre-Position and Reconfiguration of Emergency Distribution Generations under Emergency System Restoration.* In this work, the emergency system restoration actions with emergency distribution generations are run at two stages. The emergency distribution generations are firstly pre-positioned on microgrid nodes for backups at the first stage. Then, after system damage occurs, some emergency distribution generations are reconfigured to suitable nodes with the aim of maximization of system resilience and performance at the second stage. The pre-positions of emergency distribution generations sharply impact the restored level $Q_{re}$ and system resilience metric of the microgrid. Considering formulas (1) and (2), we propose the following pre-position strategy for the emergency system restoration of the microgrid.

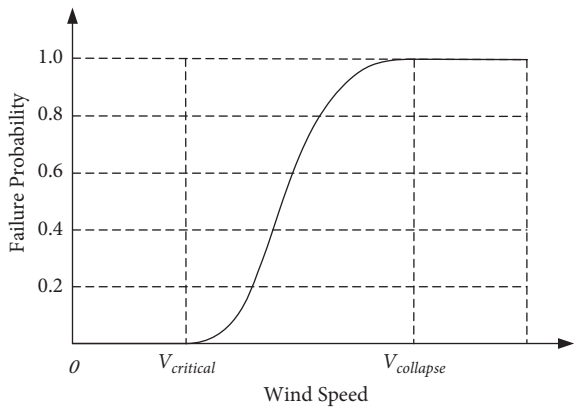


Figure 2: Fragility curve of transmission lines with failure probability as a function of wind speed.

*Definition 1.* The pre-position of distribution generation is defined by the following steps. Firstly, the nodes of the microgrid are sorted in descending order of the value of $w_i q_i^0$. Then, the emergency distribution generations are sorted in descending order of the value of $G_k$. Finally, $m$ emergency distribution generations are mapped to be pre-positioned on the previous $m$ nodes of the microgrid system.

Following the above pre-position strategy, the emergency distribution generations are inclined to be pre-positioned at the first stage on these nodes, where it has the larger weighted load demand value. At the second stage, since the damage of wind storm is uncertain, it is necessary to adjust and reconfigure the pre-positioned emergency distribution generations for better system resilience and performance. For simplicity, we assume that the pre-positioned distribution generation can be reconfigured only once, and each node can be located with two emergency distribution generations at most. So, we provide the following reconfiguration strategy.

*Definition 2.* Based on the damaged transmission lines and pre-positioned emergency distribution generations, the power output of distribution generation $k$ pre-positioned on node $j$ and shed loads on node $i$ can be determined, respectively, as $q_{k,j}^1$ and $\Delta d_i$, after optimizing the power flow of the damaged microgrid system at the first stage. Distribution generation $k$ can be reconfigured to node $z$ at the second stage as follows:

$$z = \begin{cases} \arg_i \max_{i \in RN} q_{k,i}^1, & \text{if } RN \neq \varnothing, \\ j, & \text{if } RN = \varnothing \end{cases} \tag{5}$$

where

$$RN = \left\{ i | q_{k,i}^1 = \min\{G_k, \Delta d_i\}, \quad q_{k,i}^1 > q_{k,j}^1 \right\}. \tag{6}$$

According to this reconfiguration strategy, the reconfiguration node for the pre-positioned distribution generation is chosen with a maximum of generation power output at those nodes, where it obtains larger generation power output in comparison to that at the pre-position node. If there exists no such node, the pre-positioned distribution generation will stay at the pre-position node.

We note that although this work focuses on the microgrid system, for the high dimensional power system, the dimensionality reduction method is an effective way to prepare for the restoration strategy design, such as reduced-order aggregate model for large-scale converters with inhomogeneous initial conditions in DC microgrids and reduced-order transfer function model of the droop-controlled inverter via Jordan continued-fraction expansion.

*3.3. Computation of Resilience Metric under Emergency System Restoration.* As mentioned above, the microgrid system under hazard is restored by the emergency restoration actions, where the emergency distribution generations are pre-positioned and reconfigured within two stages. This certainly affects the resilience assessment for the microgrid at the focused states, where the core issue is the computation of resilience metric under the system emergency restoration.

Assume that the performance of the microgrid system reduces to degraded level $Q_{de}$ at the degraded state. After the pre-position and reconfiguration of emergency distribution generations, the restored system performance level $Q_{re}$ can be actually determined by the OPF approach from a system view. However, the startup sequence of the pre-positioned and reconfigured emergency distribution generations still affects the resilience assessment metric of the system restoration. With consideration of system stability, the pre-positioned and reconfigured emergency distribution generations are sequentially started for energy supply at the beginning of each time interval $\Delta t$. Then, the upgraded curve in Figure 1 at the restoration state will be changed to the "staircase" curve as shown in Figure 3.

Considering the system resilience metric in formulas (1) and (2), if the pre-positioned and reconfigured distribution generation on the node with the higher value of "weighted" power demand obtains an earlier start, it will prompt the higher system performance with the above "staircase" curve and lead to the higher resilience metric under system emergency restoration. So, we provide the following startup strategy for the pre-positioned and reconfigured emergency distribution generations.

*Definition 3.* The startup sequence of emergency distribution generations is defined by the following steps. Firstly, the microgrid nodes with the pre-positioned and reconfigured emergency distribution generations are sorted in descending order of their values of $w_i q_{k,i}^1$. Then, the emergency distribution generations are sequentially started by the order of the nodes at the beginning of each time interval $\Delta t$.

Therefore, in order to compute the formulas in Section 3, we propose the following proposition.

**Proposition 1.** *Assume that the time of restoration state* $[t_{re}, t_{res}]$ *is divided into* $m+1$ *time intervals as* $\{\Delta t, \ldots, \Delta t, \Delta t_1\}$ *and* $m\Delta t + \Delta t_1 = t_{res} - t_{re}$. *During each of precious m time intervals, the system performance is upgraded* $w_i \Delta q_{k,i}^1$ $(i \in N, k \in \widehat{M})$ *by the started pre-positioned (or*

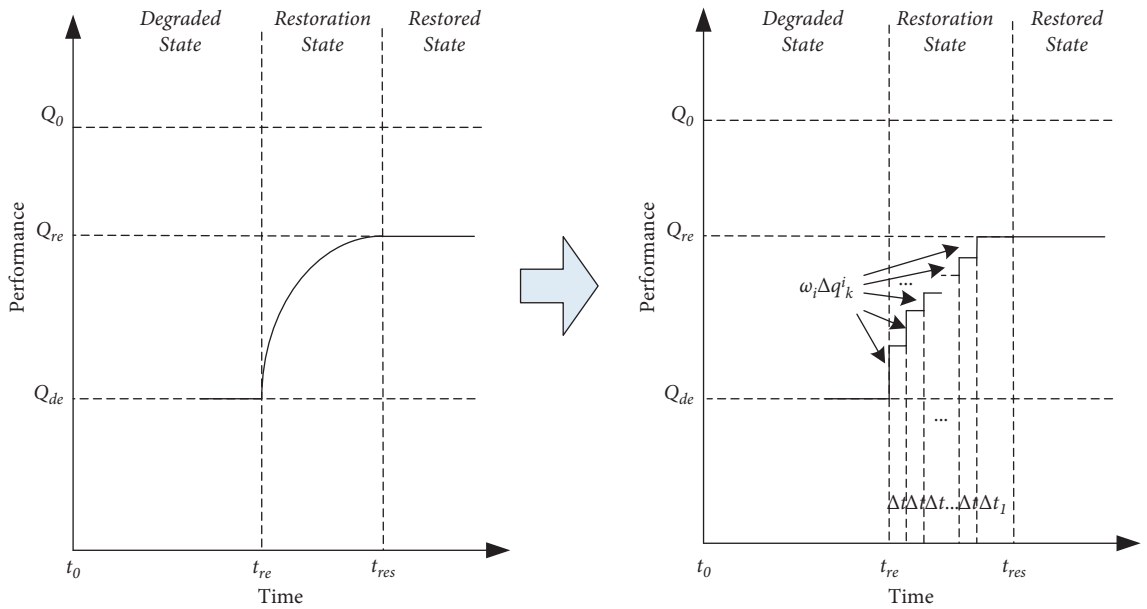


Figure 3: Performance curve of restoration state changed as a staircase.

*reconfigured) distribution generation k on node i, where $\widehat{M}$ is the new distribution generation set of startup based on Definition 3 and* $Q_{de} + \sum_{k=1}^{m} w_i \Delta q^1_{k,i} = Q_{re}$. *Then,* $\int_{t_{re}}^{t_{res}} Q^1(t)dt$ *in formula (2) can be computed as*

$$\int_{t_{re}}^{t_{\text{res}}} Q^1(t)\mathrm{d}t = Q_{de} m\Delta t + \sum_{k=1}^{m}\left(\sum_{z=1}^{z=k} w_i \Delta q^1_{z,i}\Delta t\right) + Q_{re}\Delta t_1. \quad (7)$$

*Proof.* As in Figure 3, $\int_{t_{re}}^{t_{\text{res}}} Q^1(t)\mathrm{d}t$ represents the computation of the area between system performance curve of restoration state and time axis. At the right of formula (7), $Q_{de} m\Delta t$ means the computation of the area between "$Q_{de}$" line and time axis at the precious $m\Delta t$ time intervals, $\sum_{k=1}^{m}(\sum_{z=1}^{z=k} w_i \Delta q^1_{z,i}\Delta t)$ represents the computation of the area between system performance curve of restoration state and "$Q_{de}$" line at precious $m\Delta t$ time intervals, and $Q_{re}\Delta t_1$ is the computation of the area between "$Q_{re}$" line and time axis at $\Delta t_1$ time interval. So, these three areas constitute the focused area between system performance curve of restoration state and time axis. □

*3.4. Assessment Framework for the Microgrid System with Emergency Restoration.* The proposed resilience assessment framework for the microgrid with distribution generation pre-position and reconfiguration under natural hazard (wind storm) is shown in Figure 4.

*Step 1.* Input the initial parameters and settings of the microgrid system, and use the OPF approach to assess the predisturbance system performance level $Q_0$.

*Step 2.* Utilize the fragility model to assess the state of the microgrid system under scenarios of a natural hazard (wind storm).

*Step 3.* Compute the postevent degraded system performance level $Q_{de}$ by the OPF approach.

*Step 4.* Utilize the system restoration model to obtain the pre-position, reconfiguration, and startup sequence of emergency distribution generations, according to Definitions 1, 2, and 3.

*Step 5.* Compute the restored system performance level $Q_{re}$ by the OPF approach for the microgrid at the restoration state.

*Step 6.* Compute the resilience metric of the microgrid system at the focused states following formulas (2), (3), and (7), and obtain the result of resilience assessment for the proposed problem.

## 4. Experiments

In this section, the simulation experiments for the assessment framework of the proposed approach are implemented on the modified IEEE 30-Bus system and the modified 118-Bus system. The experiments have been executed on a laptop with Intel Core i7 CPU@4 GHz and 32 GB RAM. The resilience assessment progress and the optimal power flow for the microgrid with pre-position and reconfiguration of emergency distribution generations have been solved using MATLAB software and YALMIP package.

*4.1. Case I: Modified IEEE 30-Bus System*

*4.1.1. Experiment Setup.* The proposed approach and metric are first tested based on the IEEE 30-Bus system. We design the experiments as follows. The parameters and the values used in the experiments are summarized in Table 1.

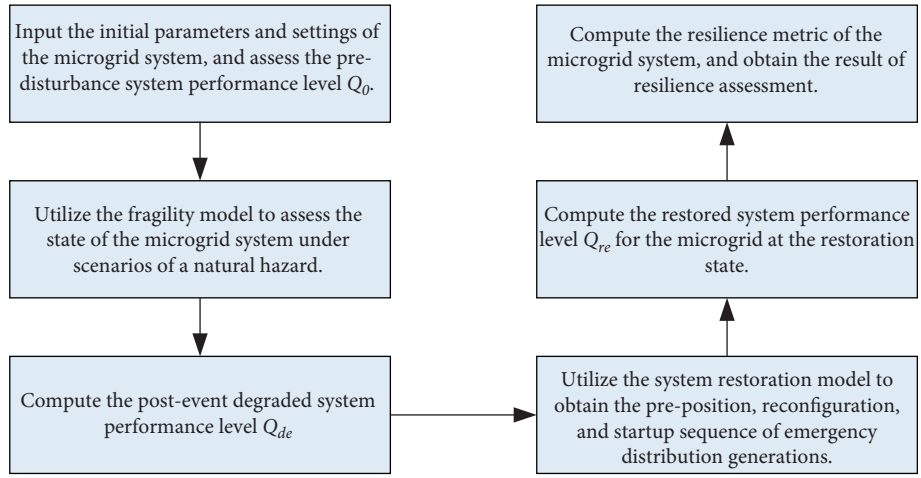


Figure 4: Resilience assessment framework for the microgrid system with emergency restoration.

Table 1: Parameters for modified IEEE 30-Bus system experiments.

| Parameter | Value, (fixed)–(varied) |
|---|---|
| Number of damaged lines | (8)–(4, 6, 8, 10, 12) |
| Times of original fixed generation capacity | (1)–(1/4, 1/2, 1, 2, 4) |
| Number ($m$) of emergency distribution generations | (4) |
| Set of distribution generation capacity | (50, 20, 20, 10) KWh |
| Set of load weight | (1, 2, 3) |
| $t_{de} - t_e$ | (1) h |
| $t_{re} - t_{de}$ | (2) h |
| $t_{ir} - t_{\text{res}}$ | (3) h |
| $t_{\text{res}} - t_{re}$ | (2) h |
| $\Delta t$ | (15) min |
| $\Delta t_1$ | (1) h |

*(1) Damaged Transmission Lines*. The damaged transmission lines in the experiments are generated according to Section 3.1. As in Table 1, the number of damaged lines varies from 4 to 12, and different damaged lines are generated. When the other parameter is focused, the number of damaged lines is fixed at 8, and the same damaged lines are used in the experiment.

*(2) Fixed Generations and Emergency Distribution Generations*. In order to investigate the effect of original generations in the IEEE 30-Bus system for the resilience assessment of microgrid under natural hazard, we have changed the capacity value from 1/4 to 4 times of that of fixed generation in the IEEE 30-Bus system. The number $m$ of emergency distribution generations is set as 4, and the capacity of 4 emergency distribution generations is, respectively, set as $\{50, 20, 20, 10\}$. We note that it is noneconomic and unnecessary to prepare the emergency distribution generations whose ability covers all the system demands. As common, we set fewer emergency distribution generations whose capacity value is larger or smaller than the average demand value of the test system case and more emergency distribution generations whose capacity value is around the average demand value.

*(3) Load Weight*. The weight of loads in the IEEE 30-Bus system is randomly generated from the set $\{1, 2, 3\}$, which means the loads are classified into three levels by their importance.

*(4) Time Length in the Focused Resilience Assessment States*. For convenient computation, we set the time length of the degradation state $[t_e, t_{de}]$, the degraded state $[t_{de}, t_{re}]$, the restoration state $[t_{re}, t_{\text{res}}]$, and the restored state $[t_{\text{res}}, t_{ir}]$, as 1 h, 2 h, 3 h, and 2 h, respectively. The time interval $\Delta t$ is set as 15 min, and $\Delta t_1$ is then set as 1 h according to Proposition 1.

*(5) Comparing System Restoration Strategies*. In the experiments, we have also provided three system restoration strategies for comparison as follows:

(i) *Strategy I (No-Restoration Strategy)*. This strategy implements no restoration action and just runs the optimal power flow on the damaged system.

(ii) *Strategy II (Pre-Position Strategy)*. It focuses on the pre-position of emergency distribution generations in the system as Definition 1 and then optimizes the power flow of the damaged system with emergency distribution generations.

(iii) *Strategy III (Pre-Position Reconfiguration Strategy)*. It first determines the pre-position of emergency distribution generations following Definition 1, then reconfigures the positioned emergency distribution generations according to Definition 2 after the damage of the system occurs, and finally optimizes the system power flow. This strategy is the proposed strategy of this paper.

*4.1.2. Experimental Result.* In this section, we present the experimental results for the resilience and performance assessment for the microgrid under natural hazard and the comparison among the different system restoration strategies. Table 2 provides the resilience and performance assessment result, and Figure 5 shows an illustrated result

Table 2: Resilience and performance assessment result with 8 damaged lines and original generations on the modified IEEE 30-Bus system.

| | Normal | Strategy I | Strategy II | Strategy III |
|---|---|---|---|---|
| Optimal running weighted loads | 389.4 | 326.4 | 350.4 | 378.9 |
| Resilience metric | — | 0.8483 | 0.9066 | 0.9432 |

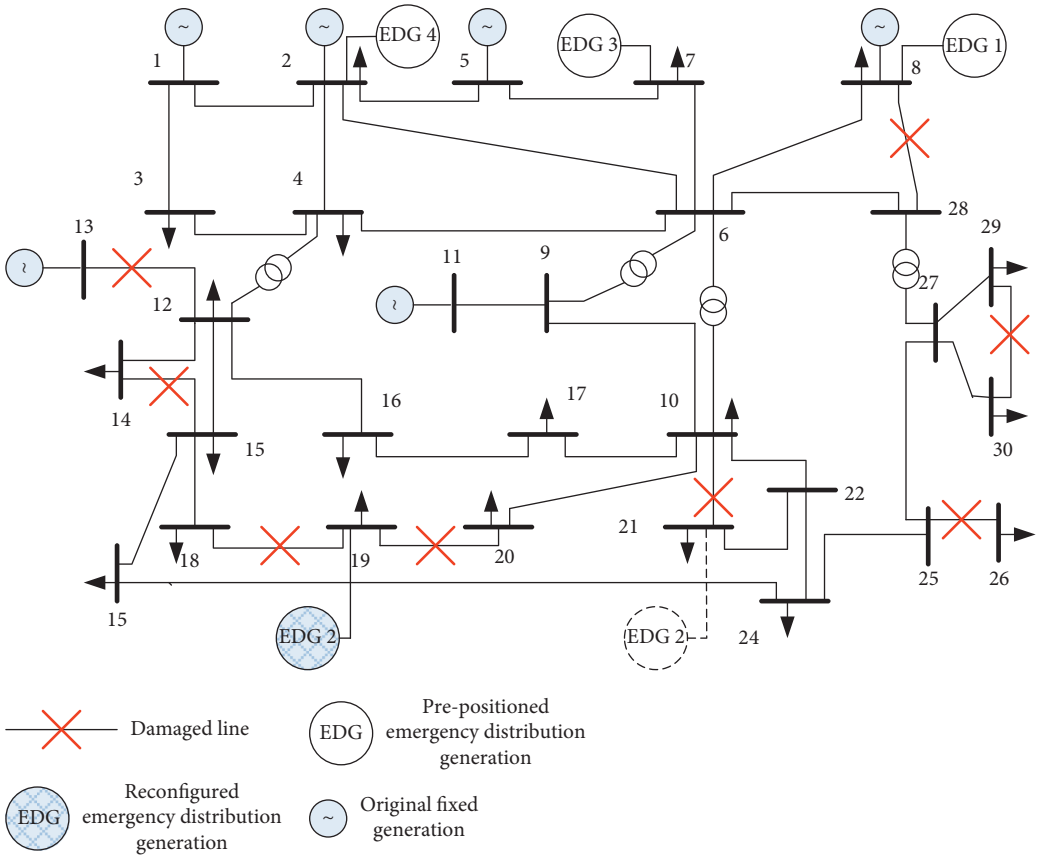


Figure 5: Illustrated restoration result under strategy III on the modified IEEE 30-Bus system.

under the proposed restoration strategy (strategy III) on the modified IEEE 30-Bus system when the number of damaged lines is set as 8 and the original fixed generations are used.

Figure 6 shows the results of optimal running weighted load and resilience metric when the same 8 damaged lines are used, and the capacities of fixed generations in the IEEE 30-Bus system are changed from 1/4 to 4 times of the original data. Figure 7 shows the results of optimal running weighted load and resilience metric when the original data of generations is used and the number of damaged lines varies from 4 to 12. Note that the "Normal" in Figures 6 and 7 means the results of optimal running weighted load and resilience metric when there is no damage in the microgrid system for a "Normal" state.

We can clearly see from Figures 6 and 7 that the optimal running weighted load of the microgrid system increases following the improvement of the capacity of fixed generations and decreases following the increment of the number of damaged lines; the resilience metric of the system with restoration actions decreases following the improvement of the capacity of fixed generations and the increment of the number of damaged lines, respectively. Particularly, when the capacity of fixed generation is not enough for power demand, the number of damaged lines is relatively larger, and the emergency distribution generations are sufficient, the reasonable restoration strategy provides a significant effect on the optimal running weighted load and system resilience metric value. This is the reason why the value of loads in Figure 6(a) under "Normal" case is smaller than strategy III at 1/4 and 1/2, and the resilience of the system decreases as the capacity of the fixed generations increases in Figure 6(b). This also confirms the effectiveness of the proposed resilience metric on the microgrid with emergency restoration under natural hazard. We can find that, based on the experiments of the modified IEEE 30-Bus system, the proposed strategy (strategy III) provides the highest value of optimal running weighted load and resilience metric when the number of damaged lines and the times of fixed generation capacity is changed, respectively. And this verifies the superiority of the proposed system restoration strategy in comparison with the other two restoration strategies.

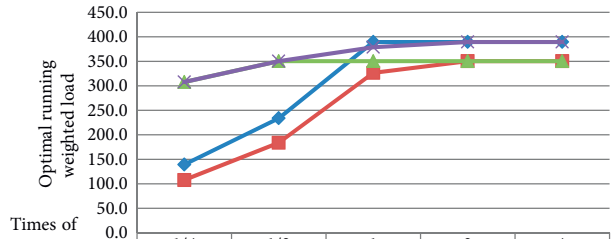


| Times of Capacity : | 1/4 | 1/2 | 1 | 2 | 4 |
|---|---|---|---|---|---|
| Normal | 139.2 | 233.8 | 389.4 | 389.4 | 389.4 |
| Strategy I | 107.7 | 183.8 | 326.4 | 350.4 | 350.4 |
| Strategy II | 307.7 | 350.3 | 350.4 | 350.4 | 350.4 |
| Strategy III | 307.7 | 350.3 | 378.9 | 389.4 | 389.4 |

(a)

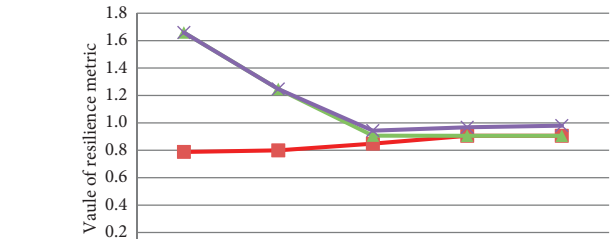


| Times of Capacity : | 1/4 | 1/2 | 1 | 2 | 4 |
|---|---|---|---|---|---|
| Strategy I | 0.7879 | 0.7995 | 0.8483 | 0.9061 | 0.9061 |
| Strategy II | 1.6589 | 1.2465 | 0.9066 | 0.9061 | 0.9061 |
| Strategy III | 1.6589 | 1.2465 | 0.9432 | 0.9679 | 0.9799 |

(b)

Figure 6: Results on modified IEEE 30 bus system with varied generation capacities.

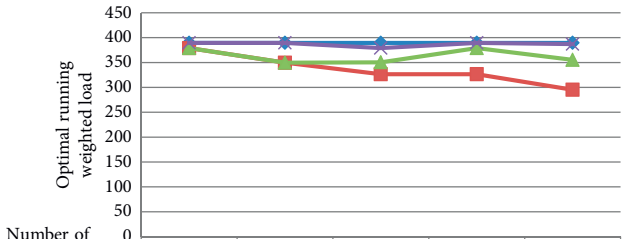


| Number of Damaged lines : | 4 | 6 | 8 | 10 | 12 |
|---|---|---|---|---|---|
| Normal | 389.4 | 389.4 | 389.4 | 389.4 | 389.4 |
| Strategy I | 378.9 | 349.7 | 326.4 | 326.4 | 295.3 |
| Strategy II | 378.9 | 349.7 | 350.4 | 378.9 | 355.3 |
| Strategy III | 389.4 | 389.4 | 378.9 | 389.4 | 387 |

(a)

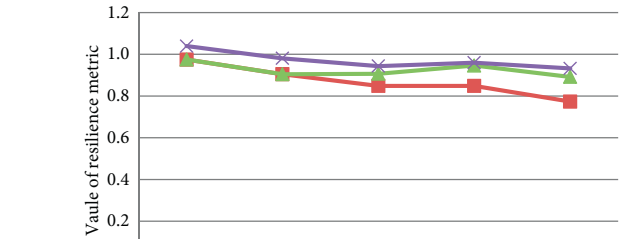


| Number of Damaged lines : | 4 | 6 | 8 | 10 | 12 |
|---|---|---|---|---|---|
| Strategy I | 0.9747 | 0.9044 | 0.8483 | 0.8483 | 0.7734 |
| Strategy II | 0.9747 | 0.9044 | 0.9066 | 0.9463 | 0.8915 |
| Strategy III | 1.0392 | 0.9806 | 0.9432 | 0.9598 | 0.9322 |

(b)

Figure 7: Results on modified IEEE 30 bus system with varied damaged lines.

### 4.2. Case II: Modified IEEE 118-Bus System

*4.2.1. Experiment Setup.* We have also tested the proposed approach and resilience metric based on the IEEE 118-Bus system. The parameters and the values used in the experiments of this section are presented in Table 3.

Like those experiment setups on the modified IEEE 30-Bus system, we have used similar settings of "load weight" and "comparing system restoration strategies" in this section. But there exist some differences: (1) the number of damaged lines varies from 10 to 40; (2) the number of emergency distribution generations is set as 10, and the capacity of 10 emergency distribution generations is, respectively, set as {100, 80, 80, 80, 50, 50, 50, 50, 20, 20}; (3) since the number of emergency distribution generations is increased to 10, the value of "$t_{\text{res}} - t_{re}$" is increased to 3 h and the value of "$\Delta t_1$" is changed as 0.5 h. Note that, as the setting of the experiment on the modified IEEE 30-Bus system, we set fewer emergency distribution generations with a larger or smaller capacity value than the average demand value of the test system case and more emergency distribution generations with the capacity value around the average demand value.

*4.2.2. Experimental Result.* Table 4 provides the performance and resilience assessment result, and Figure 8 presents an illustrated result under strategy III on the modified IEEE 118-Bus system when the number of damaged lines is set as 20 and the original fixed generation data is used.

Table 3: Parameters for modified IEEE 118-Bus system experiments.

| Parameter | Value (fixed)–(varied) |
|---|---|
| Number of damaged lines | (20)–(10, 15, 20, 30, 40) |
| Times of original fixed generation capacity | (1)–(1/4, 1/2, 1, 2, 4) |
| Number ($m$) of emergency distribution generations | (10) |
| Set of distribution generation capacity | (100, 80, 80, 80, 50, 50, 50, 50, 20, 20) KWh |
| Set of load weight | (1, 2, 3) |
| $t_{de} - t_e$ | (1) h |
| $t_{re} - t_{de}$ | (2) h |
| $t_{ir} - t_{\text{res}}$ | (3) h |
| $t_{\text{res}} - t_{re}$ | (3) h |
| $\Delta t$ | (15) min |
| $\Delta t_1$ | (0.5) h |

Figure 9 provides the results of the optimal running weighted load and system resilience metric when the similar 20 damaged lines are used and the capacities of generations in the IEEE 118-Bus system are changed from 1/4 to 4 times

Table 4: Resilience and performance assessment result with 20 damaged lines and original generations on modified IEEE 118-Bus system.

| | Normal | Strategy I | Strategy II | Strategy III |
|---|---|---|---|---|
| Optimal running weighted loads | 1293 | 1293 | 2483 | 2733 |
| Resilience metric | — | 1.0000 | 1.5682 | 1.6434 |

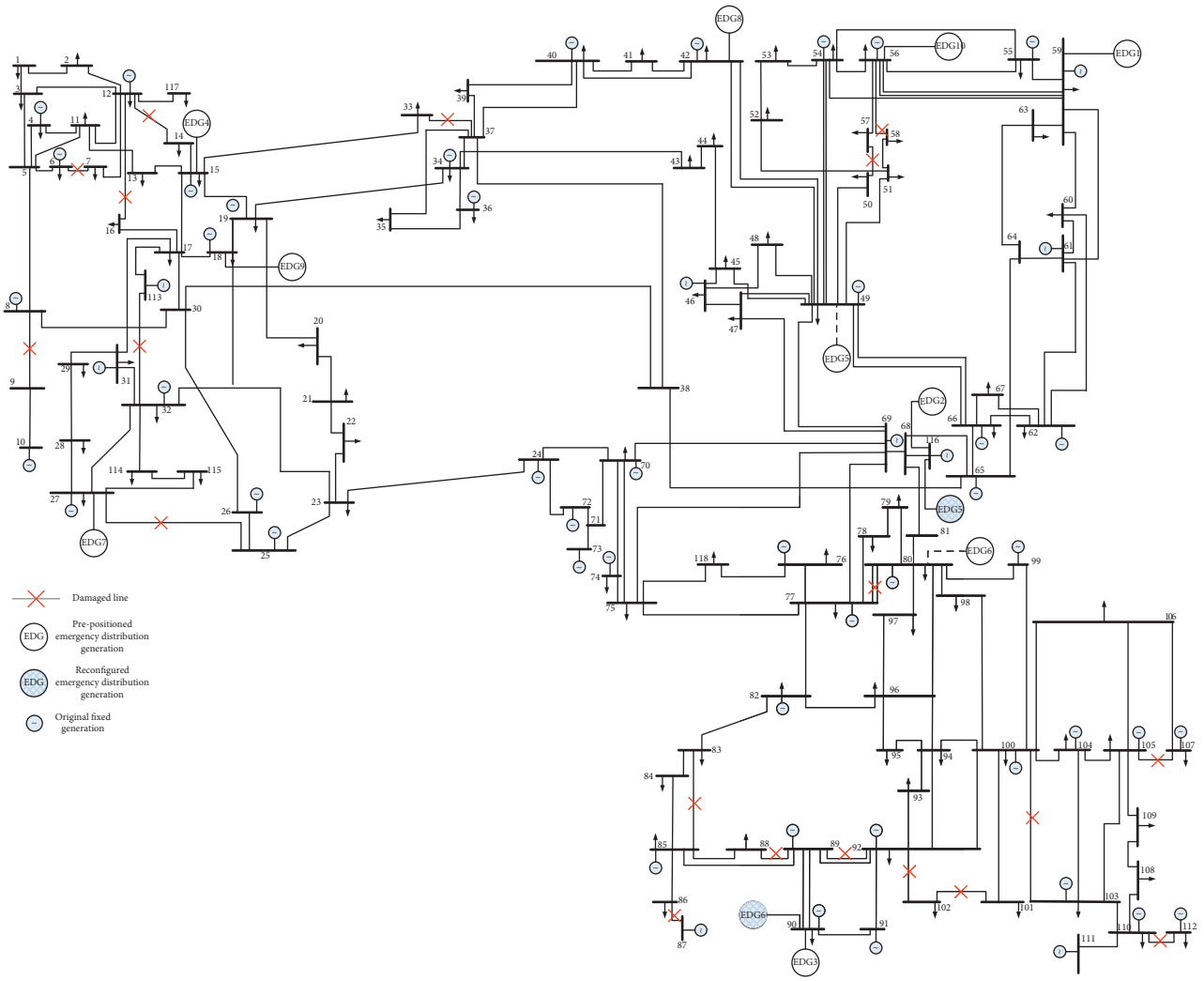


Figure 8: Illustrated restoration result under strategy III on modified IEEE 118-Bus system.

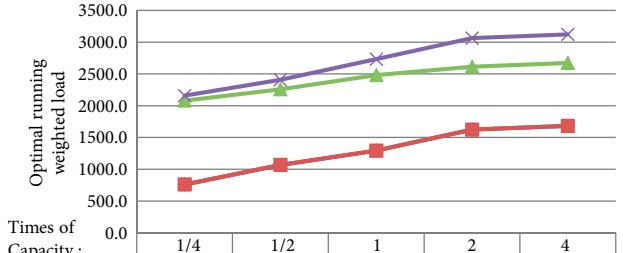


| Times of Capacity : | 1/4 | 1/2 | 1 | 2 | 4 |
|---|---|---|---|---|---|
| Normal | 760.5 | 1068.0 | 1293.0 | 1624.0 | 1683.0 |
| Strategy I | 760.5 | 1068.0 | 1293.0 | 1624.0 | 1683.0 |
| Strategy II | 2080.0 | 2258.0 | 2483.0 | 2614.0 | 2673.0 |
| Strategy III | 2158.5 | 2408.0 | 2733.0 | 3064.0 | 3123.0 |

(a)

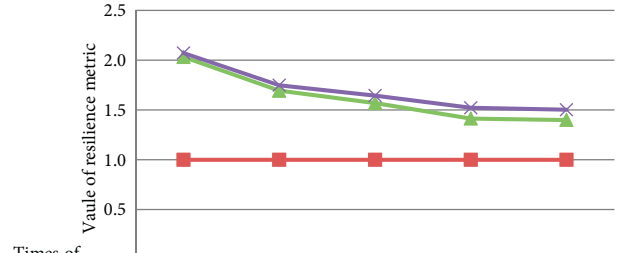


| Times of Capacity : | 1/4 | 1/2 | 1 | 2 | 4 |
|---|---|---|---|---|---|
| Strategy I | 1.0000 | 1.0000 | 1.0000 | 1.0000 | 1.0000 |
| Stratgey II | 2.0323 | 1.6931 | 1.5682 | 1.4136 | 1.3991 |
| Strategy III | 2.0725 | 1.7478 | 1.6434 | 1.5213 | 1.5031 |

(b)

Figure 9: Results on modified IEEE 118 bus system with varied generation capacities.

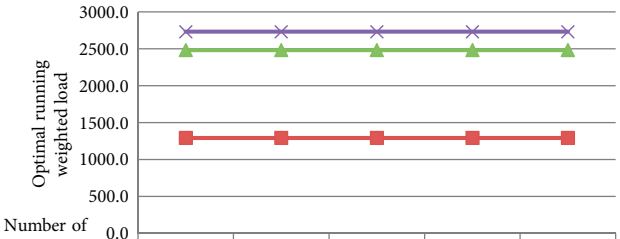


| Number of Damaged lines : | 10 | 15 | 20 | 30 | 40 |
|---|---|---|---|---|---|
| Normal | 1293.0 | 1293.0 | 1293.0 | 1293.0 | 1293.0 |
| Strategy I | 1293.0 | 1293.0 | 1293.0 | 1293.0 | 1293.0 |
| Strategy II | 2483.0 | 2483.0 | 2483.0 | 2483.0 | 2483.0 |
| Strategy III | 2733.0 | 2733.0 | 2733.0 | 2733.0 | 2733.0 |

(a)

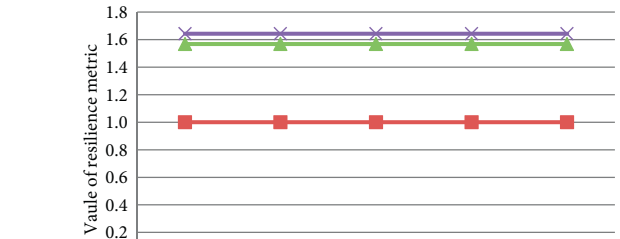


| Number of Damaged lines : | 10 | 15 | 20 | 30 | 40 |
|---|---|---|---|---|---|
| Strategy I | 1.0000 | 1.0000 | 1.0000 | 1.0000 | 1.0000 |
| Strategy II | 1.5682 | 1.5682 | 1.5682 | 1.5682 | 1.5682 |
| Strategy III | 1.6434 | 1.6434 | 1.6434 | 1.6434 | 1.6434 |

(b)

Figure 10: Results on modified IEEE 118 bus system with varied damaged lines.

of the original data. Figure 10 gives the results of the optimal running weighted load and system resilience metric when the original data of fixed generations is used and the number of damaged lines varies from 10 to 40.

From Table 4 and Figures 9 and 10, we can observe that the proposed restoration strategy also provides the highest value of optimal running weighted load and system resilience at these experiments based on the modified IEEE 118-Bus system. And we can see that the value of the system resilience metric is equal to 1 when there exists no restoration action by the generations under "strategy I." This is because there are 54 fixed generations distributed at the system with 118 buses in the original data, and these distributed generations can provide enough energy supply for the buses when the damage occurs. We can also find that the value of the system resilience metric is larger than 1 under "strategy II" and "strategy III," and this is because more energy can be supplied by suitably positioned generations, and more resiliency can be obtained by the microgrid system. Note that since there are 54 generations distributed at the 118 buses in the original data, it can achieve a "stable state" of optimal running weighted load and system resilience metric though the number of damaged lines is changed from 10 to 40 at the experiments as in Figure 10.

## 5. Conclusion

This paper introduces and solves the microgrid system resilience assessment under natural hazard, where the emergency distribution generations are pre-positioned and reconfigured on microgrid nodes for system emergency restoration. We provide a resilience metric index and an approximation computation method for the system resilience assessment, a pre-position strategy and a reconfiguration strategy of emergency distribution generations for the microgrid system restoration, and a framework of resilience assessment for problem-solving. The effectiveness of the resilience assessment methodology and the superiority of proposed restoration strategies are, respectively, verified with extensive experiments.

Since we focus on the resilience metric computation and the emergency restoration strategy of microgrid under natural hazard in this work, two directions will be considered in our future work. First, we intend to propose the mathematical formation of the multistage resilience assessment of microgrid with system emergency restoration under natural hazard. Secondly, we would like to apply our method for the resilience assessment of the sea island microgrid system, where a seasonal natural disaster occurs frequently.

## Data Availability

The data used to support the findings of this study are available from the corresponding author upon request.

## Conflicts of Interest

The authors declare that they have no conflicts of interest.

## Acknowledgments

This work was partly supported by the Chinese National Natural Science Foundation under Grants 61973310, 71901210, and 72071205. This support was greatly appreciated.

## References

[1] R. J. Campbell and S. Lowry, "Weather-related power outages and electric system resiliency," in *Proceedings of the Congressional Research Service*, Library of Congress, Washington, DC, USA, August 2012.

[2] C. S. Holling, "Resilience and stability of ecological systems," *Annual Review of Ecology and Systematics*, vol. 4, no. 1, pp. 1–23, 1973.

[3] C. Folke, "Resilience: the emergence of a perspective for social-ecological systems analyses," *Global Environmental Change*, vol. 16, no. 3, pp. 253–267, 2006.

[4] R. Francis and B. Bekera, "A metric and frameworks for resilience analysis of engineered and infrastructure systems," *Reliability Engineering and System Safety*, vol. 121, pp. 90–103, 2014.

[5] L. Mili, K. Triantis, and A. Greer, "Integrating community resilience in power system planning," *Power Engineering:*

*Advances and Challenges, Part B: Electrical Power*, CRC Press, Boca Raton, FI, USA, 2018.

[6] M. H. Amirioun, F. Aminifar, H. Lesani, and M. Shahidehpour, "Metrics and quantitative framework for assessing microgrid resilience against windstorms," *International Journal of Electrical Power and Energy Systems*, vol. 104, pp. 716–723, 2019.

[7] M. Bruneau, S. E. Chang, R. T. Eguchi et al., "A framework to quantitatively assess and enhance the seismic resilience of communities," *Earthquake Spectra*, vol. 19, no. 4, pp. 733–752, 2003.

[8] A. Dehghani, M. Sedighizadeh, and F. Haghjoo, "An overview of the assessment metrics of the concept of resilience in electrical grids," *International Transactions on Electrical Energy Systems*, vol. 31, no. 12, Article ID e13159, 2021.

[9] M. Ibrahim and A. Alkhraibat, "Resiliency assessment of microgrid systems," *Applied Sciences*, vol. 10, no. 5, p. 1824, 2020.

[10] F. H. Jufri, V. Widiputra, and J. Jung, "State-of-the-art review on power grid resilience to extreme weather events: definitions, frameworks, quantitative assessment methodologies, and enhancement strategies," *Applied Energy*, vol. 239, pp. 1049–1065, 2019.

[11] M. Ouyang and L. Dueñas-Osorio, "Time-dependent resilience assessment and improvement of urban infrastructure systems," *Chaos*, vol. 22, no. 3, pp. 033122-033123, 2012.

[12] M. Panteli, P. Mancarella, D. N. Trakas, E. Kyriakides, and N. D. Hatziargyriou, "Metrics and quantification of operational and infrastructure resilience in power systems," *IEEE Transactions on Power Systems*, vol. 32, no. 6, pp. 4732–4742, 2017.

[13] M. Bruneau and A. Reinhorn, "Exploring the concept of seismic resilience for acute care facilities," *Earthquake Spectra*, vol. 23, no. 1, pp. 41–62, 2007.

[14] S. Lei, J. Wang, C. Chen, and Y. Hou, "Mobile emergency generator pre-positioning and real-time allocation for resilient response to natural disasters," *IEEE Transactions on Smart Grid*, vol. 9, no. 3, pp. 2030–2041, 2018.

[15] B. Ti, G. Li, M. Zhou, and J. Wang, "Resilience assessment and improvement for cyber-physical power systems under typhoon disasters," *IEEE Transactions on Smart Grid*, vol. 13, no. 1, pp. 783–794, 2022.

[16] M. H. Amirioun, F. Aminifar, and H. Lesani, "Resilience-oriented proactive management of microgrids against windstorms," *IEEE Transactions on Power Systems*, vol. 33, no. 4, pp. 4275–4284, 2018.

[17] A. Hussain, V.-H. Bui, and H.-M. Kim, "Microgrids as a resilience resource and strategies used by microgrids for enhancing resilience," *Applied Energy*, vol. 240, pp. 56–72, 2019.

[18] J. Nelson, N. G. Johnson, K. Fahy, and T. A. Hansen, "Statistical development of microgrid resilience during islanding operations," *Applied Energy*, vol. 279, Article ID 115724, 2020.

[19] T. T. Dan and W. T. P. Wang, "A more resilient grid: the us department of energy joins with stakeholders in an r & d plan," *IEEE Power and Energy Magazine*, vol. 13, no. 3, pp. 26–34, 2015.

[20] Z. Bie, Y. Lin, G. Li, and F. Li, "Battling the extreme: a study on the power system resilience," *Proceedings of the IEEE*, vol. 105, no. 7, pp. 1253–1266, 2017.

[21] M. Panteli, D. N. Trakas, P. Mancarella, and N. D. Hatziargyriou, "Power systems resilience assessment: hardening and smart operational enhancement strategies," *Proceedings of the IEEE*, vol. 105, no. 7, pp. 1202–1213, 2017.

[22] R. D. Zimmerman, C. E. Murillo-Sánchez, and R. J. Thomas, "MATPOWER: steady-state operations, planning, and analysis tools for power systems research and education," *IEEE Transactions on Power Systems*, vol. 26, no. 1, pp. 12–19, 2011.

[23] M. Panteli, C. Pickering, S. Wilkinson, R. Dawson, and P. Mancarella, "Power system resilience to extreme weather: fragility modeling, probabilistic impact assessment, and adaptation measures," *IEEE Transactions on Power Systems*, vol. 32, no. 5, pp. 3747–3757, 2017.

[24] L. McColl, E. J. Palin, H. E. Thornton, R. A. Betts, K. Mylne, and M. H. S. David, "Assessing the potential impact of climate change on the UK's electricity network," *Climatic Change*, vol. 115, no. 3, pp. 821–835, 2012.

[25] G. Fu, S. Wilkinson, R. J. Dawson et al., "Integrated approach to assess the resilience of future electricity infrastructure networks to climate hazards," *IEEE Systems Journal*, vol. 12, no. 4, pp. 3169–3180, 2018.